Retina Publish Ahead of Print

DOI: 10.1097/IAE.0000000000003801

Hyperreflective band in the ganglion cell layer in retinitis pigmentosa

Antropoli Alessio[1] MD, Arrigo Alessandro[1*] MD, PhD, Bianco Lorenzo[1] MD, Cavallari Elena[1] MD, Berni Alessandro[1] MD, Casoni Filippo[2] PhD, Consalez Giacomo[2] MD, Bandello Francesco[1] MD, Cremona Ottavio[2]† MD, PhD, Battaglia Parodi Maurizio[1]† MD

[1] Department of Ophthalmology, Vita-Salute San Raffaele University, IRCCS San Raffaele Scientific Institute, Milan, Italy

[2]Università Vita-Salute San Raffaele, Milan, Italy

† Joint senior authors

[*]Corresponding Author:

Alessandro Arrigo

IRCCS San Raffaele Scientific Institute, Department of Ophthalmology

Via Olgettina, 60, Milan, Lombardy, 20132, Italy

Tel: +39 340 077 8477

E-mail: arrigo.alessandro@hsr.it

Financial Support: none

Acknowledgements: Supported by Progetto di Ricerca Finalizzata Ministero della Salute NET2016.

Conflict of interest: no conflict of interest exists for any author

Abbreviated title: Hyperreflective GCL band in Retinitis Pigmentosa

KEYWORDS AND SUMMARY STATEMENT

Keywords: Retinitis pigmentosa, ganglion cells, ganglion cell layer, optical coherence tomography, inherited retinal disease

Summary statement: The hyperreflective ganglion cell layer band is an OCT finding characterizing approximately a quarter of retinitis pigmentosa eyes and is associated with a poorer visual function.

ABSTRACT

Purpose: To describe a sign that takes the form of a continuous hyperreflective band within the thickness of the ganglion cell layer (GCL), thus dubbed the "hyperreflective ganglion cell layer band" (HGB), which we detected in a fraction of patients affected by retinitis pigmentosa (RP).

Methods: Retrospective, cross-sectional, observational study. Optical coherence tomography (OCT) images of RP patients examined between May 2015 and June 2021 were retrospectively reviewed for the presence of HGB, epiretinal membrane (ERM), macular hole and cystoid macular edema (CME). The ellipsoid zone (EZ) width was also measured. A subgroup of patients underwent microperimetry in the central 2°,4° and 10°.

Results: One hundred forty-four eyes from 77 subjects were included in the study. HGB was present in 39 (25.3%) RP eyes. Mean best-corrected visual acuity (BCVA) was 0.39 ± 0.05 logMAR (approximately 20/50 Snellen equivalent) and 0.18 ± 0.03 logMAR (approximately 20/32 Snellen equivalent) in eyes with and without HGB, respectively ($p < 0.001$). The two groups did not differ with regard to EZ width, mean 2°, 4° and 10° retinal sensitivity, and prevalence of CME,

ERM and macular hole. The multivariable analysis showed the presence of HGB to be a predictor of poorer BCVA ($p<0.001$).

Conclusions: HGB is an OCT finding detectable in approximately a quarter of RP eyes and is associated with a poorer visual function. In the discussion, we speculate about possible morphogenetic scenarios to explain this observation.

INTRODUCTION

Retinitis pigmentosa (RP) is a group of inherited retinal dystrophies characterized by progressive rod-cone photoreceptor degeneration, resulting in vision loss.[1] Following the degenerative changes in the photoreceptors, various secondary changes occur in the retina, including Müller cell gliosis and migration of retinal pigmented epithelium (RPE) toward the inner retina.[2] However, even after photoreceptor degeneration, the inner retinal layers may be spared to a certain extent. These preserved structures undergo retinal remodeling, followed by transneuronal degeneration over their natural history.[3–5] The rarity of the disease makes it difficult to obtain histological samples and there are therefore few histological studies of human retinas.[3,5] On the other hand, modern optical coherence tomography (OCT) has proved an invaluable tool for detecting such retinal changes and monitoring disease progression, enabling non-invasive, high resolution *in vivo* retinal imaging to be performed.[6–8]

Thanks to this technique, changes in retinal microstructure involving the thinning of the retinal layers, first in the outer retina and then in the inner, can be viewed.[6] At the same time, the thickness

of the ganglion cell layer (GCL), inner plexiform layer (IPL) and retinal nerve fiber layer (RNFL) remains unchanged or even increases in the earlier stages.[6,9–11] It is important to acquire information regarding the time frame of retinal degeneration and the status of the ganglion cells (GCs) themselves, as these elements will likely influence the success of emerging treatments, especially optogenetic therapy.[1,6,12]

In the present study, we identified a sign in a fraction of RP patients we termed "hyperreflective GCL band" (HGB). This sign consists of a continuous hyperreflective band within the thickness of the GCL, as detected by spectral-domain (SD) OCT. This led us to speculate on possible structural alterations underlying HGB and their clinical impact.

METHODS

This was a retrospective, cross-sectional, observational study. We identified RP patients followed at the Heredodystrophy Unit of the Ophthalmology Department of IRCCS San Raffaele Hospital from May 2015 to June 2021. We ensured they satisfied the inclusion criteria, and collected clinical and OCT data from their first available visit. We included RP patients with at least a radial and a raster image for both eyes. Exclusion criteria were: any other ocular disorder, poor quality images due to high media opacity or extensive vitreous floaters and/or the presence of RPE atrophy in the macular region, in at least one eye.

Structural OCT images were acquired with a Spectralis HRA+OCT (Heidelberg Engineering, Heidelberg, Germany). The standard acquisition protocol consisted of at least a radial pattern of six B-scans, with a 30° angle and a high number of frames (ART>25), and a raster pattern of nineteen 20° angle B-scans (ART > 9) spaced 234 µm apart. Best-corrected visual acuity (BCVA) was collected using a standard ETDRS chart.

OCT images were reviewed for the presence of HGB, defined as a continuous hyperreflective band within the thickness of the GCL, with no sign of of a shadow effect produced by retinal vessels.[13] This feature was most clearly observable in the parafoveal region, where the GCL is physiologically thicker than in the rest of the retina.[14] A few small gaps in the hyperreflective band were allowed, as long as the HGB continuity was clearly maintained (Figures 1 and 2). Each image was carefully reviewed for the presence of HGB by two masked graders (A.A. and L.B.). In cases of disagreement, a third grader (A.B.) was consulted and his conclusions were used for the analyses. RP patients were compared with an age-, gender- and refraction-matched healthy control group and reviewed for the presence of HGB.

OCT scans were also reviewed for the presence of common RP comorbidities, such as epiretinal membrane (ERM), macular hole and cystoid macular edema (CME). ERM was defined on OCT as irregular, hyperreflective lines above the inner retinal surface, often causing retinal wrinkling with hyporeflective spaces between the ERM and the internal limiting membrane.[15] Ectopic inner foveal layers (EIFL), which could present on OCT as hyperreflective band crossing the foveal region and originating from the inner nuclear layer extending from the inner nuclear layer (INL) and IPL, were identified and distinguished from HGB.[15] Cystoid macular edema (CME) was defined as hyporeflective cystic spaces on two or more consecutive macular raster scans.[23]

Lastly, we measured ellipsoid zone (EZ) width on horizontal and vertical radial scans. Values ranged from the total scan length (when EZ width exceeded the total length of the OCT scan) to a minimum value of 0 µm (when EZ was not distinguishable).

When available, retinal sensitivity (RS) measurements obtained in mesopic conditions with the Macular Integrity Assessment (MAIA) microperimeter (CenterVue, Padua, Italy) were collected. The grid selected for the study had 68 Goldman III-sized stimuli spaced 2° apart and set 10° from the fixation point. The patient was asked to fixate a 1° diameter red ring against a background of 1.27 cd/m2 (4 asb), while achromatic stimuli were presented using a 4-2 full threshold projection

scheme. The intensity of the light projected ranged from 1 to 0.25 asb, equivalent to 0 and 36 dB. Patients underwent 15-minutes of dark adaptation and pupil dilation with 1% Tropicamide prior to the examination. Each eye was tested separately by occluding the fellow eye. We recorded mean RS values of the central 4, 12 and 68 points, approximately corresponding to the central 2°, 4° and 10°, respectively. Tests exceeding 30% of fixation losses and eyes with an undetectable EZ were excluded.

Disease-causing mutations were identified from each patient's medical history, and their relative frequencies were recorded. Whenever a causal gene could not be identified, we labeled the case as "unsolved".

Statistical analysis

Analyses were performed using SPSS Statistics 23 (IBM; Armonk, NY). All descriptive data were expressed as mean ± standard deviation (SD) for continuous variables and as frequency and percentages for categorical ones. Continuous variable normality was assessed using the Kolmogorov-Smirnov test. Age and sex were compared between patients without HGB and subjects exhibiting HGB in at least one eye. Age was compared with the two-sample Student's t-test. Frequencies among groups were compared with the chi-square test. A generalized linear mixed-effect regression model was adopted for BCVA, RS and EZ width comparison to account for inter-eye correlations, and the HGB variable was selected as fixed effect. For the same reason, we used a two-level mixed-effect linear model to investigate the relationship between BCVA (dependent variable) and the presence of HGB, CME, ERM, macular hole, EZ widths, and age (predictor variables, level 1) nested within patients (level 2). Predictors significantly associated with BCVA in univariable analysis were included in the multivariable regression model. The effect on the outcome of one unit change in the predictor variable was reported as beta coefficient (β), 95% confidence intervals, and p-value.

Inter-observer agreement for the presence of HGB was determined with Cohen's kappa statistic. Kappa results were interpreted as either weak (0.40-0.59), moderate (0.60-0.79), strong (0.80-0.90), or almost perfect (>0.90).[16] We also calculated the estimated prevalence of the HGB with its corresponding 95% confidence interval (CI). All tests were two-sided, and the level of significance was set at $p < 0.05$.

RESULTS

One hundred eighty-two eyes from 91 patients were considered for the study. Fourteen patients were excluded because one presented with a choroidal neovascularization, 4 patients had RPE atrophy, and 9 patients had poor quality images due to media opacities. In the end, 144 eyes from 77 subjects were included in the study. Forty-two (54.5%) subjects were female. The control group consisted of 74 eyes of 37 sex-, age- and refraction-matched healthy subjects. The patients' demographics are summarized in Table 1.

HGB appeared on OCT B-scans as a hyperreflective band in the GCL, without posterior shadowing effect, and was most recognizable in the parafoveal region. In RP patients, HGB was present in 39 (25.3%) eyes and absent in 115 (74.7%) eyes (Figure 3), while it was absent in all (0%) healthy controls. A strong intergrader agreement with a kappa coefficient of 0.83 ($p < 0.001$) was reached in the RP group, and it was a perfect 0.00 ($p < 0.001$) in the control group. More specifically, 6 (3.9%) cases required the appraisal of the third grader, who confirmed the presence of the HGB in 5 of those.

The estimated prevalence of HGB in RP was 25.3% (95% CI: 18.7-33.0; $p < 0.001$). HGB was bilateral in 18 (23.4%) patients, unilateral in 3 (3.9%) patients, and absent in 56 (72.7%) subjects.

Mean BCVA was 0.39 ± 0.05 logMAR (approximately corresponding to 20/50 Snellen equivalent; 95% CI: 0.3-0.49), and 0.18 ± 0.03 logMAR (approximately corresponding to 20/32 Snellen

equivalent; 95% CI: 0.12-0.23) in eyes with and without HGB, respectively ($p < 0.001$). The mean age of onset of RP, based on the visual symptoms reported, was 23.59 ± 15.27 and 30.79 ± 14.0 (not reaching statistical significance), in patients displaying and not displaying HGB, respectively.

Twenty-seven patients underwent microperimetry, three of whom were excluded because unable to complete the test. RS values were recorded for 48 eyes from 24 patients. The two groups did not differ in terms of mean 2°, 4° and 10° RS ($p = 0.519$, 0.364, 0.531, respectively). Moreover, horizontal and vertical EZ width ($p = 0.359$ and 0.325, respectively), and the prevalence of CME, ERM and macular holes also proved to be comparable (Table 1).

In the univariable regression model, the predictors significantly associated with BCVA were HGB, EZ widths, and age, while in the multivariable mixed model only the presence of HGB had a significant impact on BCVA: patients showing this feature had a worse BCVA (0.39 ± 0.05 logMAR, approximately 20/50 Snellen equivalent) than those without (0.18 ± 0.03; $p<0.001$). All data are reported in Table 2.

All patients underwent genetic testing, but a causal gene could not be identified in 21 (27.3%) of cases. The relative frequencies of each disease-causing mutation are reported in Supplementary Table S1, http://links.lww.com/IAE/B968. The most common pathogenetic variant was USH2A, present in 25 (44.6%) out of 56 patients. However, no clear correlation was found between HGB presence and genetic characterization. The prevalence of HGB in relation to the causal gene is reported in Supplementary Table S2, http://links.lww.com/IAE/B968.

DISCUSSION

The inner layers of the human retina contain numerous cell types other than GCs, including amacrine cells (ACs), astroglial cells, and Müller cell bodies, as well as including most of the superficial vascular plexus (SVP).[17,18] Notably, astrocytes are mostly confined to the nerve fiber

layer and GCL, and can be subdivided according to their morphology into stellate, bipolar and perivascular astrocytes, with the last of these surrounding the blood vessels of the SCP in the GCL.[19]

Histological studies of the retinas of RP patients have revealed a substantial preservation of the GCL until the later stages of the disease, when, following photoreceptor death, the transneuronal degeneration causes a severe reduction of the GCs.[3,5] On OCT, only changes happening in the later stages of the disease were observed, such as a thinning of the inner retinal layers, with direct consequences for BCVA and retinal sensitivity.[6,11,20]

In this study, we describe the HGB as a new feature of the GCL, found by OCT in approximately a quarter of the patients affected by RP. We define it as a continuous hyperreflective band that is fully enclosed in the GCL, bilaterally in almost all cases, becoming more frequent in females. Neither EZ width nor the prevalence of comorbidities differed between patients with and without HGB. Moreover, our data indicate that the presence of HGB on structural OCT is an independent visual function indicator in patients affected by RP.

Previous studies have identified processes of retinal remodeling in the inner retina that involve both cells of the GCL and the retinal microvasculature.[5] RPE cell migration toward the vessels of the inner retina, which is the histological correlate of the "bone spicules" in RP, is one of the most typical and best described features.[21] Furthermore, a thick layer of extracellular matrix (ECM), whose composition closely resembles Bruch's membrane, surrounds retinal capillaries and venules in RP.[21] Another important retinal remodeling process in RP consists of astrocytes and Müller cell gliosis.[2]

Studies on rat RP models found that astrocyte processes, which are closely associated with retinal vessels of the SCP, are hypertrophic.[22] In RP retinas, Müller cells undergo reactive gliosis as well. This process, together with an increased expression of growth factors and other changes in the retinal homeostasis in RP, is thought to be the cause of the neurite sprouting from rods to the inner

retinal layers.[23,24] Even though neurite sprouting from rods has not been observed in the macula of these patients, there is evidence that other cell types behave similarly in RP. A study by Fariss et al. found that both amacrine and horizontal cells sprout neurites associated with the surface of gliotic Müller cells toward the inner layers in human RP retinas.[25] We hypothesize that neurite sprouting from cells of the inner retina, astrocyte gliosis, and/or microvascular changes of the superficial capillary plexus (SCP) may contribute to the development of HGB visible with OCT in RP patients.

Nevertheless, it is hard to explain why HGB should appear in just a fraction of RP patients. Notably, RP development in animal models shows the occurrence of different patterns of reactive gliosis and GCL involvement, depending upon the pathogenic factors implicated. (i) In the RP rat model with the P23H opsin mutation (P23H rat), there is a spontaneous development of a moderate reactive gliosis of the astrocyte-type in the GCL, which is peaking at 18 months of age.[22] (ii) In this very same rat model, the onset of RP and related gliosis can be dramatically accelerated by intravitreal administration of ATP; notably, the gliosis induced by ATP is peaking at six months of age, and it is characterized by a massive proliferation of astrocytes in the GCL in comparison with untreated P23H rats of the same age.[26] The pathogenetic action of ATP is not fully understood, but there is a general consensus that its neurotoxicity is exerted through purinergic receptors, mainly P2X7R,[27] which is expressed in several components of the retinal layers, including photoreceptor cells (as initially observed), retinal ganglion cells, amacrine and horizontal cells, microglia and Müller glial cells, astrocytes and pericytes as well as RPE cells.[28,29] A large body of evidence suggests the involvement of P2X7R in neurodegenerative diseases, including Alzheimer disease.[30] The stimulation of P2X7R causes a release of pro-inflammatory cytokines and ROS by microglia and macrophages, contributing to neuroinflammation,[31] a factor tightly related to the onset and progression of RP.[32] Strikingly, expression of P2X7R and P2X4R (another purinergic receptor involved in neurodegeneration)[33] are upregulated in a different rodent model of RP, the rd10 mouse.[34] (iii) In the P23H rat model, the onset of RP and related gliosis can also be dramatically accelerated by eliciting a mild chronic inflammation through systemic injection of

lipopolysaccharides (LS); remarkably, the gliosis induced by LS is mainly of the Müller cell-type, and affects several retinal layers with a mild thickening of the GCL.[35] LPS possibly act through an entirely different pathogenic pathway, i.e. microglial activation through Toll-like receptor 4 (TLR4), which triggers the production and release of pro-inflammatory cytokines, such as interleukin (IL)-1β, IL-6, and Tumor necrosis factor alpha (TNF-α), by the Mitogen-activated protein kinase (MAPK) and Nuclear factor kappa beta (NF-kβ) routes.[35]

Based on (i) the three patterns of GCL reactive gliosis described above, (ii) the continuous aspect of HGB, with minor interruptions (often represented by transversally sectioned vessels casting a shadowing effect), and (iii) the observed increase of astrocyte density from the peripheral to the central region of the retina,[22] which aligns with the observation that HGB is more easily visible in the parafoveal region, reactive gliosis of the aforementioned perivascular astrocytes of the GCL seems the most reasonable hypothesis to explain the morphological aspect of HCB. Furthermore, the different effect of RP pathogenic factors on GCL gliosis may explain its occurrence in a restricted subset of RP patients.

We hypothesize that the changes resulting in the manifestation of HGB on OCT may be attributed to specific genetic influences. Patients carrying more severe genetic alterations may experience deeper cell degeneration and transformation. Unfortunately, the small sample size in the present study prevented the association between the presence of HGB and distinct genotypes being assessed. A multicenter study on a much larger cohort of RP patients might address this point in the future.

An intriguing aspect of our results concerns the discrepancies in visual acuity in eyes showing HGB in association with a preserved retinal sensitivity. Even though RS and BCVA are correlated, the former is the expression of complex retinal cell interactions, while the latter depends on the integrity of the foveal center, and changes in one parameter are not necessarily followed by

modifications of the other.[36] The cone dysfunction may be attributed to the microglial activation in RP secondary to rod degeneration.[37,38]

The advent of OCT-angiography (OCTA) paved the way for in vivo studies of the retinal microvasculature and its perfusion, which has revealed an almost constant reduction of the vessel density of the DCP, while data on the SCP are more controversial.[17,39] In a recent study, Nassisi et al. found that in areas where the outer retina is spared, vessel density is normal.[40] Conversely, Villegas-Perez et al. proposed a mechanism of GC "death" that involved the cells' compression by the abnormal retinal vessels.[41] In our view, it is possible that patients with a relatively preserved GCL have a less compromised SCP, while the GCs of patients showing HGB may be experiencing cellular stress and reactive gliosis due to the vascular abnormalities, and that the presence of this OCT sign may be a biomarker of gliosis and/or SCP proliferation. This hypothesis needs to be verified by OCTA – which was not included in our study – in order to ascertain if there is a reduction of the vessel density of the SCP in patients with HGB.

Lastly, all our patients had undergone genetic testing, and we could identify a pathogenetic variant responsible for the disease in roughly two-thirds of the cases, which is consistent with the diagnostic yield previously reported in the literature.[42,43] Nonetheless, as already mentioned, the limited sample size precluded us from finding any association between the presence of HGB and any specific genotype.

Additionally, the retrospective and cross-sectional design of our study is a further limitation, as it restricts our ability to gather data regarding the exact timing of HGB development and the age of symptom onset for each patient, and the lack of histological samples renders the interpretation of our results merely speculative.

Even so, we should like to put HGB forward as a new OCT finding visible in approximately a quarter of RP eyes. It is associated with a poorer visual function, possibly resulting from processes of gliosis and neurite sprouting around the capillaries of the SCP. Further research on larger cohorts

of genetically ascertained RP patients will provide longitudinal data and focus on histopathological and OCTA correlates of HGB.

References

1. Verbakel SK, van Huet RAC, Boon CJF, et al. Non-syndromic retinitis pigmentosa. *Prog Retin Eye Res*. 2018;66:157-186. doi:10.1016/j.preteyeres.2018.03.005

2. Milam AH, Li ZY, Fariss RN. Histopathology of the human retina in retinitis pigmentosa. *Prog Retin Eye Res*. 1998;17(2):175-205. doi:10.1016/s1350-9462(97)00012-8

3. Santos A, Humayun MS, de Juan E, et al. Preservation of the inner retina in retinitis pigmentosa. A morphometric analysis. *Arch Ophthalmol*. 1997;115(4):511-515. doi:10.1001/archopht.1997.01100150513011

4. Gartner S, Henkind P. Pathology of Retinitis Pigmentosa. *Ophthalmology*. 1982;89(12):1425-1432. doi:10.1016/S0161-6420(82)34620-5

5. Stone JL, Barlow WE, Humayun MS, et al. Morphometric analysis of macular photoreceptors

and ganglion cells in retinas with retinitis pigmentosa. *Arch Ophthalmol*. 1992;110(11):1634-1639. doi:10.1001/archopht.1992.01080230134038

6. Yoon CK, Bae K, Yu HG. Longitudinal Microstructure Changes of the Retina and Choroid in Retinitis Pigmentosa. *American Journal of Ophthalmology*. 2022;241:149-159. doi:10.1016/j.ajo.2022.05.002

7. Aizawa S, Mitamura Y, Baba T, et al. Correlation between visual function and photoreceptor inner/outer segment junction in patients with retinitis pigmentosa. *Eye (Lond)*. 2009;23(2):304-308. doi:10.1038/sj.eye.6703076

8. Liu G, Liu X, Li H, et al. Optical Coherence Tomographic Analysis of Retina in Retinitis Pigmentosa Patients. *Ophthalmic Res*. 2016;56(3):111-122. doi:10.1159/000445063

9. Hood DC, Lin CE, Lazow MA, et al. Thickness of receptor and post-receptor retinal layers in patients with retinitis pigmentosa measured with frequency-domain optical coherence tomography. *Invest Ophthalmol Vis Sci*. 2009;50(5):2328-2336. doi:10.1167/iovs.08-2936

10. Vámos R, Tátrai E, Németh J, et al. The Structure and Function of the Macula in Patients with Advanced Retinitis Pigmentosa. *Investigative Ophthalmology & Visual Science*. 2011;52(11):8425-8432. doi:10.1167/iovs.11-7780

11. Yoon CK, Yu HG. Ganglion cell-inner plexiform layer and retinal nerve fibre layer changes within the macula in retinitis pigmentosa: a spectral domain optical coherence tomography study. *Acta Ophthalmol*. 2018;96(2):e180-e188. doi:10.1111/aos.13577

12. Lindner M, Gilhooley MJ, Hughes S, Hankins MW. Optogenetics for visual restoration: From proof of principle to translational challenges. *Prog Retin Eye Res*. 2022;91:101089. doi:10.1016/j.preteyeres.2022.101089

13. Willerslev A, Li XQ, Cordtz P, et al. Retinal and choroidal intravascular spectral-domain optical coherence tomography. *Acta Ophthalmol*. 2014;92(2):126-132. doi:10.1111/aos.12048

14. Remington LA, ed. *Clinical Anatomy and Physiology of the Visual System (Third Edition)*. Butterworth-Heinemann; 2012. doi:10.1016/B978-1-4377-1926-0.10031-1

15. Govetto A, Lalane RA, Sarraf D, et al. Insights Into Epiretinal Membranes: Presence of Ectopic Inner Foveal Layers and a New Optical Coherence Tomography Staging Scheme. *Am J Ophthalmol*. 2017;175:99-113. doi:10.1016/j.ajo.2016.12.006

16. McHugh ML. Interrater reliability: the kappa statistic. *Biochem Med (Zagreb)*. 2012;22(3):276-282.

17. Campbell JP, Zhang M, Hwang TS, et al. Detailed Vascular Anatomy of the Human Retina by Projection-Resolved Optical Coherence Tomography Angiography. *Sci Rep*. 2017;7(1):42201. doi:10.1038/srep42201

18. Levin, Leonard, Nilsson S, Ver Hoeve J, et al. *Adler's Physiology of the Eye*. 11th Edition. Levin Leonard; 1993.

19. Reichenbach A, Bringmann A. Glia of the human retina. *Glia*. 2020;68(4):768-796. doi:10.1002/glia.23727

20. Arrigo A, Aragona E, Perra C, et al. Morphological and functional involvement of the inner retina in retinitis pigmentosa. *Eye (Lond)*. Published online June 29, 2022. doi:10.1038/s41433-022-02139-7

21. Li ZY, Possin DE, Milam AH. Histopathology of bone spicule pigmentation in retinitis pigmentosa. *Ophthalmology*. 1995;102(5):805-816. doi:10.1016/s0161-6420(95)30953-0

22. Fernández-Sánchez L, Lax P, Campello L, et al. Astrocytes and Müller Cell Alterations During Retinal Degeneration in a Transgenic Rat Model of Retinitis Pigmentosa. *Front Cell Neurosci*. 2015;9:484. doi:10.3389/fncel.2015.00484

23. Li ZY, Kljavin IJ, Milam AH. Rod photoreceptor neurite sprouting in retinitis pigmentosa. *J*

Neurosci. 1995;15(8):5429-5438. doi:10.1523/JNEUROSCI.15-08-05429.1995

24. Gao H, Hollyfield JG. Basic fibroblast growth factor: increased gene expression in inherited and light-induced photoreceptor degeneration. *Exp Eye Res*. 1996;62(2):181-189. doi:10.1006/exer.1996.0022

25. Fariss RN, Li ZY, Milam AH. Abnormalities in rod photoreceptors, amacrine cells, and horizontal cells in human retinas with retinitis pigmentosa. *Am J Ophthalmol*. 2000;129(2):215-223. doi:10.1016/s0002-9394(99)00401-8

26. Calzaferri F, Ruiz-Ruiz C, de Diego AMG, et al. The purinergic P2X7 receptor as a potential drug target to combat neuroinflammation in neurodegenerative diseases. *Medicinal Research Reviews*. 2020;40(6):2427-2465. doi:10.1002/med.21710

27. Adinolfi E, Giuliani AL, De Marchi E, et al. The P2X7 receptor: A main player in inflammation. *Biochem Pharmacol*. 2018;151:234-244. doi:10.1016/j.bcp.2017.12.021

28. Reichenbach A, Bringmann A. Purinergic signaling in retinal degeneration and regeneration. *Neuropharmacology*. 2016;104:194-211. doi:10.1016/j.neuropharm.2015.05.005

29. Vessey KA, Fletcher EL. Rod and Cone Pathway Signalling Is Altered in the P2X7 Receptor Knock Out Mouse. *PLOS ONE*. 2012;7(1):e29990. doi:10.1371/journal.pone.0029990

30. Francistiová L, Bianchi C, Di Lauro C, et al. The Role of P2X7 Receptor in Alzheimer's Disease. *Frontiers in Molecular Neuroscience*. 2020;13. Accessed March 2, 2023. https://www.frontiersin.org/articles/10.3389/fnmol.2020.00094

31. Di Virgilio F, Dal Ben D, Sarti AC, et al. The P2X7 Receptor in Infection and Inflammation. *Immunity*. 2017;47(1):15-31. doi:10.1016/j.immuni.2017.06.020

32. Zhao L, Hou C, Yan N. Neuroinflammation in retinitis pigmentosa: Therapies targeting the innate immune system. *Frontiers in Immunology*. 2022;13. Accessed March 2, 2023.

https://www.frontiersin.org/articles/10.3389/fimmu.2022.1059947

33. Castillo C, Saez-Orellana F, Godoy PA, Fuentealba J. Microglial Activation Modulated by P2X4R in Ischemia and Repercussions in Alzheimer's Disease. *Frontiers in Physiology*. 2022;13. Accessed March 2, 2023. https://www.frontiersin.org/articles/10.3389/fphys.2022.814999

34. Martínez-Gil N, Kutsyr O, Noailles A, et al. Purinergic Receptors P2X7 and P2X4 as Markers of Disease Progression in the rd10 Mouse Model of Inherited Retinal Dystrophy. *International Journal of Molecular Sciences*. 2022;23(23):14758. doi:10.3390/ijms232314758

35. Noailles A, Maneu V, Campello L, et al. Systemic inflammation induced by lipopolysaccharide aggravates inherited retinal dystrophy. *Cell Death Dis*. 2018;9(3):1-18. doi:10.1038/s41419-018-0355-x

36. Iftikhar M, Kherani S, Kaur R, et al. Progression of Retinitis Pigmentosa as Measured on Microperimetry: The PREP-1 Study. *Ophthalmol Retina*. 2018;2(5):502-507. doi:10.1016/j.oret.2017.09.008

37. Narayan DS, Wood JPM, Chidlow G, Casson RJ. A review of the mechanisms of cone degeneration in retinitis pigmentosa. *Acta Ophthalmol*. 2016;94(8):748-754. doi:10.1111/aos.13141

38. Peng B, Xiao J, Wang K, et al. Suppression of microglial activation is neuroprotective in a mouse model of human retinitis pigmentosa. *J Neurosci*. 2014;34(24):8139-8150. doi:10.1523/JNEUROSCI.5200-13.2014

39. Battaglia Parodi M, Cicinelli MV, Rabiolo A, et al. Vessel density analysis in patients with retinitis pigmentosa by means of optical coherence tomography angiography. *Br J Ophthalmol*. 2017;101(4):428-432. doi:10.1136/bjophthalmol-2016-308925

40. Nassisi M, Lavia C, Mohand-Said S, et al. Near-infrared fundus autofluorescence alterations correlate with swept-source optical coherence tomography angiography findings in patients with retinitis pigmentosa. *Sci Rep*. 2021;11(1):3180. doi:10.1038/s41598-021-82757-5

41. Villegas-Pérez MP, Vidal-Sanz M, Lund RD. Mechanism of retinal ganglion cell loss in inherited retinal dystrophy. *Neuroreport*. 1996;7(12):1995-1999. doi:10.1097/00001756-199608120-00028

42. Ellingford JM, Barton S, Bhaskar S, et al. Whole Genome Sequencing Increases Molecular Diagnostic Yield Compared with Current Diagnostic Testing for Inherited Retinal Disease. *Ophthalmology*. 2016;123(5):1143-1150. doi:10.1016/j.ophtha.2016.01.009

43. Neveling K, Collin RWJ, Gilissen C, et al. Next-generation genetic testing for retinitis pigmentosa. *Hum Mutat*. 2012;33(6):963-972. doi:10.1002/humu.22045

FIGURE LEGENDS

Figure 1 - Radial Pattern B-Scans of a 25-year-old female patient with retinitis pigmentosa showing a continuous hyperreflective band in the ganglion cell layer.

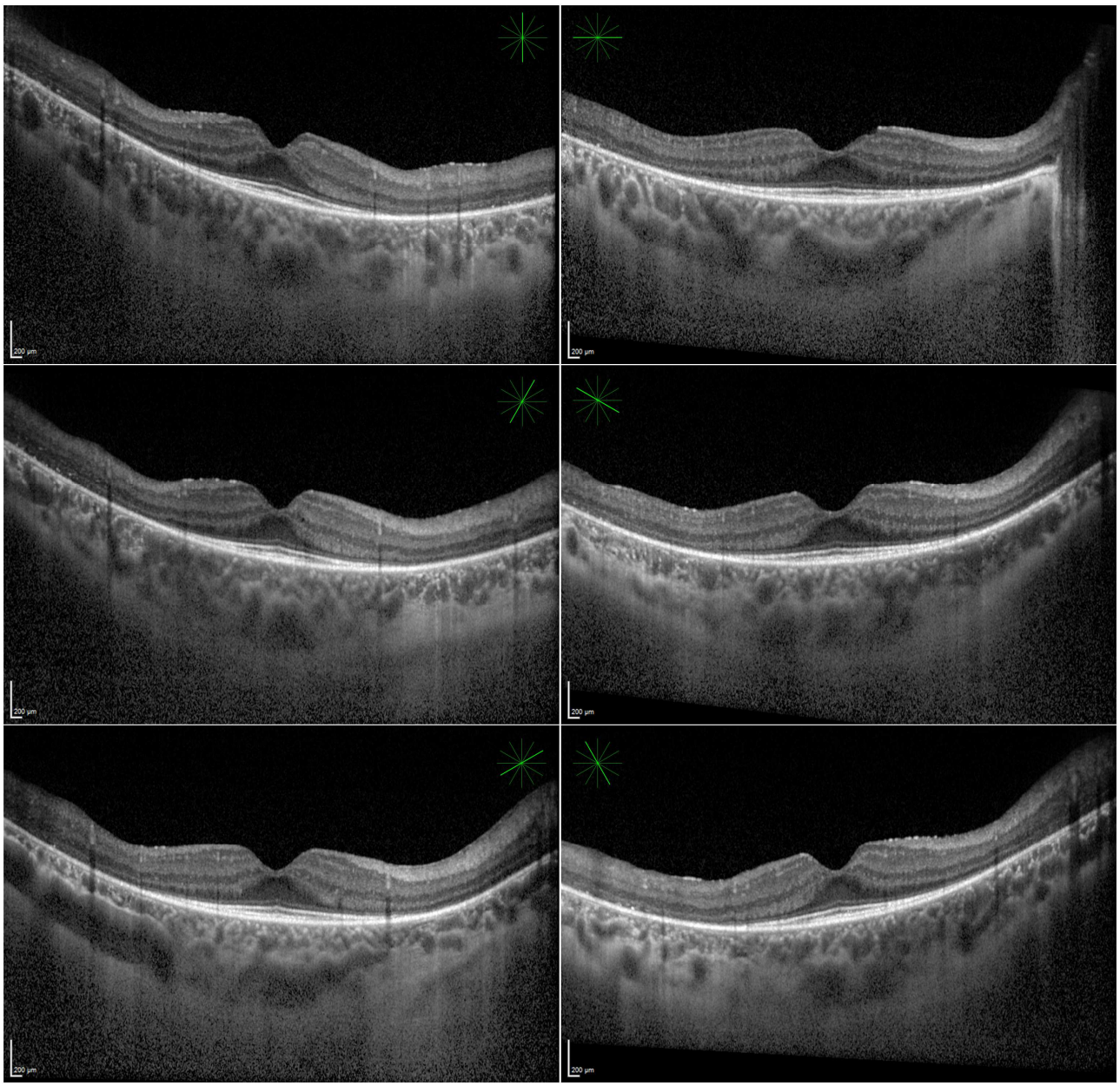

Figure 2 - Close-up of a parafoveal OCT scan of a female 18-year-old patient. The HGB is visible as a continuous layer (yellow arrowheads) in the ganglion cell layer.

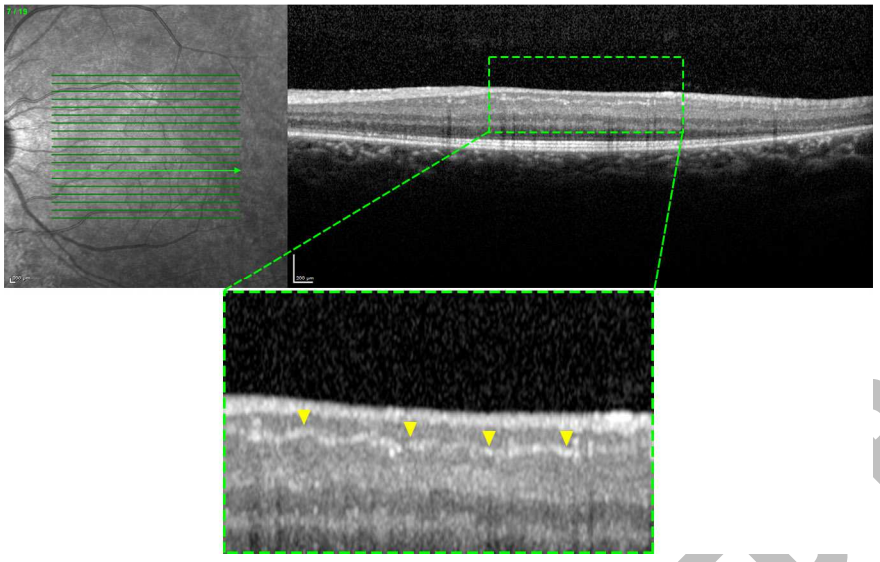

Figure 3 – OCT scans from three patients with HGB (upper row) and three subjects without (lower row).

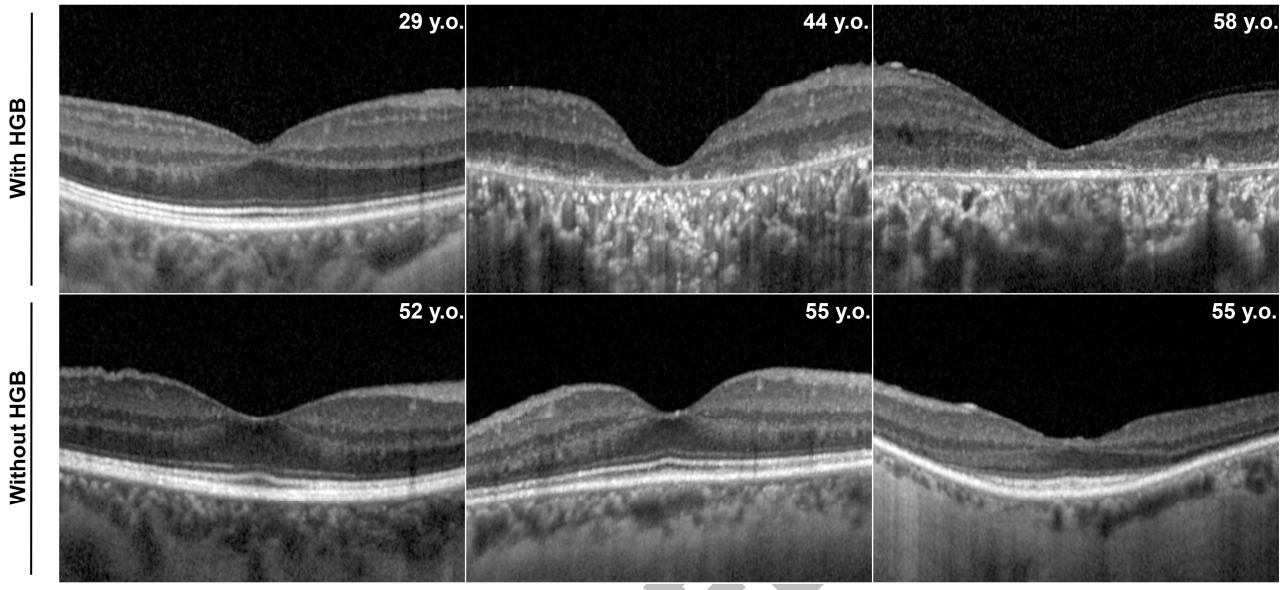

Table 1. Comparison between patients and eyes with and without HGB

	Patients with HGB (21)	**Patients without HGB (56)**	**p value**
Sex (n, %)	16 (76.2)	26 (46.4)	**0.019**
Age (Years, mean ± SD)	36.72 ± 14.06	38.45 ± 15.36	0.608
Age of onset (Years, mean ± SD)	30.79 ± 14.00	23.59 ± 15.27	0.097
	Eyes with HGB (39)	**Eyes without HGB (115)**	
BCVA (logMAR, mean ± SD)	0.39 ± 0.05	0.18 ± 0.03	**<0.001**
EZ width horizontal (µm, mean ± SD)	3315 ± 241	2874 ± 414	0.359
EZ width vertical (µm, mean ± SD)	2957 ± 243	2479 ± 418	0.325
CME (n, %)	9 (23.1)	26 (25.2)	0.952
ERM (n, %)	25 (64.1)	56 (48.7)	0.096
Macular Hole (n, %)	0 (0)	4 (3.5)	0.238
	Eyes with HGB (13)	**Eyes without HGB (35)**	

RS 2° (dB, mean ± SD)	22.7 ± 3.7	23.6 ± 3.7	0.519
RS 4° (dB, mean ± SD)	17.6 ± 8.5	19.7 ± 6.3	0.364
RS 10° (dB, mean ± SD)	10.5 ± 7.6	12.2 ± 8.7	0.531
P values for Student's t-test, generalized mixed model effect regression test and Chi-Square test, as appropriate. RP = retinitis pigmentosa; HGB = hyper-reflective ganglion cell layer bands; SD = standard deviation; BCVA = best-corrected visual acuity; EZ = ellipsoid zone; RS = retinal sensitivity.			

Table 2. Two-level linear mixed-effect model regression of clinical and imaging predictors of BCVA

	Univariable analyses			**Multivariable analyses**		
	Beta coefficient (logMAR)	**95% CI (Lower limit – Upper limit)**	**p value***	**Beta coefficient (logMAR)**	**95% CI (Lower limit – Upper limit)**	**p value***
HGB	0.14	0.02 – 0.25	**0.024**	0.14	0.03 – 0.25	**0.014**
EZ width horizontal (µm)	$-2.55E^{-5}$	$-4.25E^{-5}$ – $-8.56E^{-6}$	**0.003**	$-2.61E^{-5}$	$-6.75E^{-5}$ – $1.54E^{-5}$	0.215
EZ width vertical (µm)	$-2.02E^{-5}$	$-3.52E^{-5}$ – $-5.07E^{-6}$	**0.009**	$2.83E^{-6}$	$-3.42E^{-5}$ – $3.98E^{-5}$	0.879
Age (years)	$0.04E^{-1}$	$0.01E^{-2}$ – 0.01	**0.042**	$0.04E^{-1}$	$-8.78E^{-2}$ – 0.01	0.055
CME	0.04	-0.05 – 0.13	0.365	-	-	-
ERM	-0.01	-0.07 – 0.05	0.761	-	-	-
Macular Hole	0.11	-0.36 – 0.26	0.137	-	-	-

Dependent variable: BCVA. *Statistically significant values in bold. BCVA = best-corrected visual acuity; CI = confidence interval; HGB = hyper-reflective ganglion cell layer band; EZ = ellipsoid zone; CME = cystoid macular edema; ERM = epiretinal membrane.

